

# A Novel Adaptive Inertia Strategy in Large-Scale Electric Power Grids

Julian Fritzsich and Philippe Jacquod

**Abstract**—The increasing penetration of new renewable sources of energy in today’s power grids is accompanied by a decrease in available electromechanical inertia. This leads to a reduced dynamical stability. To counterbalance this effect, virtual synchronous generators have been proposed to emulate conventional generators and provide inertia to power systems. The high flexibility of these devices makes it possible to control the synthetic inertia they provide and to have them operate even more efficiently than the electromechanical inertia they replace. Here, we propose a novel control scheme for virtual synchronous generators, where the amount of inertia provided is large at short times – thereby absorbing local faults and disturbances as efficiently as conventional generators – but decreases over a tunable time interval to prevent long-time coherent oscillations from setting in. This new model is used to investigate the effect of adaptive inertia on large-scale power grids. Our model outperforms conventional constant inertia in all scenarios and for all performance measures considered. We show how an optimized geographical distribution of adaptive inertia devices not only effectively absorbs local faults, but also significantly improves the damping of inter-area oscillations.

## I. INTRODUCTION

The energy sector is the main contributor to global carbon dioxide emissions [1]. This motivates the currently ongoing push toward decarbonization of power generation, including a strong increase in penetration of new renewable energy sources (NRE) in electric power systems. NRE differ from traditional power plants in at least three fundamental ways. First, they are volatile and have more fluctuating, less predictable power productions. Second, they are geographically decentralized. Third, they are connected to the grid via electronic power converters, and thus have altogether different dynamics from standard power plants with electromechanically coupled rotating machines. Increasing the penetration of NRE in power grids therefore implies significant reduction in availability of ancillary services such as electromechanical inertia with a simultaneous increase in power fluctuations.

This poses new challenges to grid operators [2]. Indeed it is well known that a decrease in inertia increases both the maximum rate of change of frequency (RoCoF) and the nadir – *i.e.*, the maximal frequency excursion – following a fault in the system, and to degraded system recovery performances [3]. Increased penetrations of NRE have been shown to result in amplified RoCoFs [4]. Operational data

for the Irish power grid additionally indicate that a decrease in inertia leads to a larger standard deviation of the system frequency [5]. Multiple solutions have been proposed to increase the stability of low-inertia grids. Among them are virtual synchronous generators (VSG) that aim to reproduce the dynamics of the swing equations [6], [7]. When connected to external electric energy storage, the VSG can emulate inertia by injecting amounts of additional active power proportional to the RoCoF. One advantage of these controllers is that their inertia is not a physical constant as in conventional generators, in particular it can be adapted to the state of the system to improve its performances. Such control schemes go by the name of *adaptive inertia*. In that spirit, Ref. [7] suggests changing the droop coefficient of the power-frequency control loop with the RoCoF, which increases the virtual inertia provided in large RoCoF events. Another adaptive inertia strategy tries to minimize the RoCoF and frequency deviation using an on-line optimization of inertia and damping constants [8]. Other control strategies change the inertia and damping proportional to the RoCoF [9]. Refs. [10], [11] propose a bang-bang control strategy which is focused on returning to the synchronized state as quickly as possible. The method has however been found to display instabilities [12], [13]. Finally, adding a power feedback loop to the virtual inertia is proposed in [14] to keep the RoCoF within predefined bounds.

These investigations focused on the response to faults and fluctuations of small grids, with few individual machines (virtual or not). In this paper we follow an altogether different approach and investigate a novel adaptive inertia scheme in large-scale power grids. Our approach is tailored to explore regimes of clear time-scale separation, which allows us to assess the impact of adaptive inertia not only on short-distance RoCoF phenomena, but also on long-range coherent inter-area oscillations. We use a simplified model of VSGs and propose a new adaptive inertia control scheme. It is based on a differential equation incorporating a driving force increasing inertia at a rate proportional to the absolute value of the RoCoF and a restoring force which brings the system back to an initial, low amount of inertia. The motivation behind the two terms is that we want first, to increase the inertia in cases of large RoCoFs to quickly mitigate its impact, and second, to re-synchronize the system fast, once the RoCoF has been sufficiently damped – this is achieved thanks to the restoring force. We investigate the impact of replacing conventional generators by such VSGs. The performance of this novel adaptive inertia scheme is measured in terms of frequency and RoCoF based  $l_2^2$  norms, the resynchronization time, and the inertial energy supplied

This work has been supported by the Swiss National Science Foundation under grant 200020\_182050.

J. Fritzsich and Ph. Jacquod are with the Department of Quantum Matter Physics, University of Geneva, CH-1211 Geneva, Switzerland and the School of Engineering, University of Applied Sciences of Western-Switzerland, CH-1950 Sion, Switzerland

Emails: julian.fritzsich@etu.unige.ch,  
philippe.jacquod@unige.ch

to the grid. We find that our adaptive scheme outperforms the standard constant inertia both in cases in which there is a change of power on either a VSG or a conventional generator. We stress that our adaptive inertia scheme in the case of a power loss is able to synchronize at an intermediate frequency value, thanks to its absence of dependence on frequency deviation. Finally, numerical results suggest that adaptive inertia VSG should be located in peripheral zones in priority.

The paper is organized as follows. Section II introduces our mathematical notation and Section III our model. Section IV investigates the stability of the extended swing equations. In Section V we investigate the performance of the extended model on two grids. First, the IEEE RTS-96 grid is used to demonstrate the impact of the different parameters of the driving and restoring force and to visualize the effect of the adaptive inertia. Second, we use a model of the European high-voltage power grid to investigate the effect of the adaptive inertia on a strongly-connected large-scale grid. We motivate why the impact of the adaptive inertia on the performance is largest when it is located in the peripheral areas. Finally, in Section VI we conclude the paper.

## II. MATHEMATICAL NOTATION

We denote vectors with lower-case bold letters and matrices with upper case bold letters. The  $i$ th component of a vector  $\mathbf{a}$  is written  $a_i$ . Diagonal matrices are denoted  $\mathbf{A} = \text{diag}(a_i)$ , where  $a_i$  is the  $i$ th diagonal element.  $\mathbf{0}$  and  $\mathbf{1}$  are the zero and identity matrix of appropriate size, respectively.  $\mathbf{0}_n$  denotes the zero vector of size  $n$ . Finally, the  $i$ th unit vector with the  $i$ th component being one and all the other components being zero is given by  $\delta_{ij}$ .

## III. MODEL

We use the swing equations to describe generation nodes. In the lossless line approximation they read [15], [16]

$$m_i \dot{\omega}_i + d_i \omega_i = P_i - \sum_j b_{ij} \sin(\theta_i - \theta_j), \quad (1)$$

where  $m_i$  is the inertia of the  $i$ th generator,  $d_i$  is the damping,  $\theta_i$  is the voltage angle,  $\omega_i = \dot{\theta}_i$  is the deviation of the frequency from the synchronized state, and  $b_{ij}$  is the product of the susceptance of the line between nodes  $i$  and  $j$  with the voltage magnitudes at nodes  $i$  and  $j$ . For load nodes we use the structure preserving model which is given by [17]

$$d_i \omega_i = P_i - \sum_j b_{ij} \sin(\theta_i - \theta_j), \quad (2)$$

where  $d_i$  in this case determines the frequency dependence of the load.

If the index  $i$  refers to a VSG, eq. (1) is augmented by

$$\dot{m}_i = \alpha_i |\dot{\omega}_i| - \beta_i (m_i - m_{\min,i}). \quad (3)$$

Eq. (3) expresses our novel adaptive inertia scheme. An important feature is that, because it does not depend on  $\omega$ , it is able to synchronize at an intermediate frequency value. The scheme depends on the minimal amount  $m_{\min,i} > 0$  of

inertia present at all time and on two control parameters  $\alpha_i$  and  $\beta_i$  whose value has to be determined to optimize system performance. The gain  $\alpha_i > 0$  controls the initial increase and the maximum amount of inertia, while  $\beta_i > 0$  controls the restoring force and with it the rate at which the inertia returns to its minimal amount. The two parameters need to be balanced to optimally absorb large RoCoF values and to quickly return to the steady state.

## IV. STABILITY

We prove that our scheme does not introduce any instability in the system, contrary to the bang-bang scheme [12], [13]. Eq. (3) cannot be linearized about the synchronous state as the derivative of  $|\dot{\omega}|$  is not defined at  $\dot{\omega} = 0$ . To examine the linear stability of the system we introduce a small deadband  $\varepsilon$  into eq. (3) without changing the fixed point as follows

$$\dot{m}_i = \frac{1}{2} \alpha_i (|\dot{\omega}_i + \varepsilon| + |\dot{\omega}_i - \varepsilon|) - \beta_i (m_i - m_{\min,i}) - \alpha_i \varepsilon, \quad (4)$$

where  $0 < \varepsilon \ll 1$ . For  $\varepsilon \rightarrow 0$  we recover the original equations. This mathematical trick allows us to linearize eqs. (1)–(3) about a fixed point with  $\omega_i = \delta\omega$ ,  $\theta_i = \theta_i^0 + \delta\theta_i$ ,  $m_i = m_{\min,i} + \delta m_i$ ,  $P = P_i^0 + \delta P_i$ . Without loss of generality, we assume that there are only generator nodes with adaptive inertia. The linearized equations then read

$$\begin{bmatrix} \delta \dot{\theta} \\ \delta \dot{\omega} \\ \delta \dot{m} \end{bmatrix} = \begin{bmatrix} \mathbf{0} & \mathbf{1} & \mathbf{0} \\ -\mathbf{M}_m^{-1} \mathbf{L} & -\mathbf{M}_m^{-1} \mathbf{D} & \mathbf{0} \\ \mathbf{0} & \mathbf{0} & -\beta \end{bmatrix} \begin{bmatrix} \delta \theta \\ \delta \omega \\ \delta m \end{bmatrix} + \begin{bmatrix} \mathbf{0} \\ \delta \mathbf{P} \\ \mathbf{0} \end{bmatrix}, \quad (5)$$

where  $\delta \theta_i = \delta \theta_i$ ,  $\delta \omega_i = \delta \omega_i$ ,  $\delta m_i = \delta m_i$ ,  $\mathbf{M}_m = \text{diag}(m_{\min,i})$ ,  $\mathbf{D} = \text{diag}(d_i)$ ,  $\beta = \text{diag}(\beta_i)$ ,  $\delta \mathbf{P}_i = \delta P_i$ , and  $\mathbf{L}$  is the network Laplacian defined as

$$\mathbf{L}_{ij} = \begin{cases} -b_{ij} \cos(\theta_i^0 - \theta_j^0) & \text{for } i \neq j, \\ b_{ij} \sum_j \cos(\theta_i^0 - \theta_j^0) & \text{for } i = j. \end{cases} \quad (6)$$

For  $n$  generators there are  $2n$  right eigenvectors of the form  $[\mathbf{u}_A^T, \mathbf{0}_n^T]^T$  with corresponding eigenvalue  $\lambda_A$ , where  $\mathbf{u}_A$  and  $\lambda_A$  are the right eigenvectors and -values of

$$\mathbf{A} = \begin{bmatrix} \mathbf{0} & \mathbf{1} \\ -\mathbf{M}_m^{-1} \mathbf{L} & -\mathbf{M}_m^{-1} \mathbf{D} \end{bmatrix}. \quad (7)$$

$\mathbf{A}$  is the stability matrix of a system with conventional generators that have inertia  $m_{\min,i}$ . Its modes are therefore stable. The remaining  $n$  eigenvectors are given by  $\mathbf{u}_j = \delta_{ij}$  for  $j \in [2n+1, 3n]$  with corresponding eigenvalue  $\lambda_j = -\beta_k < 0$  where  $k = j - 2n$ . We conclude that the small signal stability of the system is the same as the stability of a system of conventional generators. There are just additional damped real modes that are located on the nodes equipped with the adaptive inertia scheme.

## V. APPLICATIONS

We evaluate the efficiency of the proposed control scheme by investigating the frequency response following a step

change in the active power injected by a conventional generator or a VSG. The four performance measures considered are the  $l_2^2$  norms of the frequency and of the RoCoF

$$l_2^2(\omega) = \sum_i \int_0^\infty (\omega_i(t) - \omega_{\text{sync}})^2 dt, \quad (8)$$

$$l_2^2(\dot{\omega}) = \sum_i \int_0^\infty \dot{\omega}_i(t)^2 dt, \quad (9)$$

the energy injected into the grid by the inertial response

$$E_{\text{rot}} = - \sum_i \int_0^\infty m_i(t) \dot{\omega}_i(t) dt, \quad (10)$$

and the resynchronization time, which we define as the time until the deviation of the frequency from the synchronous state is less than 1 mHz on all nodes. As we argue below, these four performance measures are sensitive to very diverse dynamical features – from short-time, fast frequency disturbances, to long-time, large-scale coherent inter-area oscillations. Optimizing our adaptive inertia scheme with respect to each four of them, if at all possible, guarantees an overall optimal disturbance mitigation protocol.

We briefly discuss the expected influence of  $\alpha_i$  and  $\beta_i$  in eq. (3) on the performance measures. Eq. (3) makes it clear that the large RoCoF following a fault increases the inertia until the RoCoF is sufficiently small or the inertia sufficiently large that the second term on its right-hand side dominates the first term. The short time behavior is therefore dominantly impacted by  $\alpha_i$ , and the long term behavior by  $\beta_i$ . Next, the frequency performance measure, eq. (8), is strongly influenced by sustained oscillations and therefore by the long-time behavior, while the RoCoF performance measure, eq. (9), is mostly determined by the short-time dynamics directly following the fault, with slow sustained oscillations having a smaller impact. Also, the resynchronization time is by definition linked to the long time system dynamics. Putting all this together, we expect the frequency and the resynchronization time performance measures to improve with increasing  $\beta_i$ , whereas the RoCoF performance measure should improve with  $\alpha_i$ . Finally, the injected energy performance measure, eq. (10), is harder to anticipate, as it depends both on the RoCoF and the inertia, which influence each other through eqs. (1) and (3).

We compare the performance measures for networks with and without VSGs. The networks considered are the IEEE RTS-96 network [18] and *PanTaGruEl*, a model of the European high voltage power grid [19], [20].

#### A. IEEE RTS-96

We begin by investigating the IEEE RTS-96 test case. The network is shown in Fig. 1. It is partitioned into three areas with ten generation units each. In the default case all of those units are conventional generators. For evaluation of our method we promote two of the generation units in each area to VSGs with the adaptive inertia method, eq. (3). The remaining nodes are loads. The inertia of the conventional generators is randomly drawn from a uniform distribution

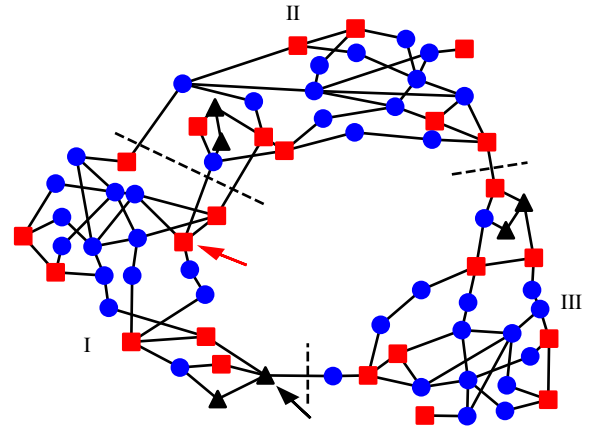


Fig. 1. The IEEE RTS-96 network. The red squares are conventional generators, the black triangles are VSGs with the adaptive inertia method, and the blue circles are load nodes. The black arrow indicates the VSG where the power is changed and the red arrow indicates the conventional generator at which a fault is applied. The roman numerals label the different areas and the dashed lines indicate their boundaries.

with  $m_i \in [0.1 \text{ pu}, 1.1 \text{ pu}]$  and the damping is chosen such that the ratio  $d_i/m_i \approx 0.3 \text{ pu}$ . For the adaptive generators the initial inertia  $m_{\text{min}}$  is set to one third of the randomly drawn inertia in the default case. We simulate an instantaneous change in the power of  $-1 \text{ pu}$  on the VSG with adaptive inertia marked by a black arrow in Fig. 1, with all VSGs having the same choice of parameters.

Fig. 2 shows the ratio of the four performance measures with and without VSGs. Panels a), b) and d) confirm our above expectations that frequency and resynchronization time performances measures improve with  $\beta$ , while the RoCoF performance measure improves with  $\alpha$ . Panel b) further shows that  $l_2^2(\dot{\omega})$  has only a weak dependence on  $\beta$  when the latter is small. This is so, because if  $\beta$  is smaller than some critical value, generator oscillations persist longer. Next, the data in panel a) depend on the ratio  $\alpha/\beta$  and not individually on  $\alpha$  nor  $\beta$ . We found that this is so, because fixing  $\alpha/\beta$  gives similar time profiles for  $m(t)$ , with in particular the same maximal inertia value. Increasing  $\alpha$  and  $\beta$  while keeping their ratio fixed gives a faster rise of virtual inertia, which does not affect the long-time dynamics. It therefore leaves  $l_2^2(\omega)$  mostly unchanged. It is remarkable that the injected energy performance measure exhibits the same behavior as  $l_2^2(\omega)$ . This suggests that it is dominated by long-term dynamical effects. Finally, the resynchronization time exhibits a more intricate behavior, with an optimal performance at large  $\alpha$  and medium  $\beta$  instead of  $\beta \gg \alpha$  as expected. We found that this behavior, however, depends on the fault location and even more on the network considered. Overall, the best global performances are obtained for both  $\alpha, \beta \gg 1$ . We therefore investigate dynamical effects in some more detail for  $\alpha = \beta = 5 \text{ pu}$ .

Fig. 3 illustrates the dynamics of the faulted generator, for the constant inertia case (black curve) and the case with homogeneous VSGs with  $\alpha = \beta = 5 \text{ pu}$  (red curve). First,

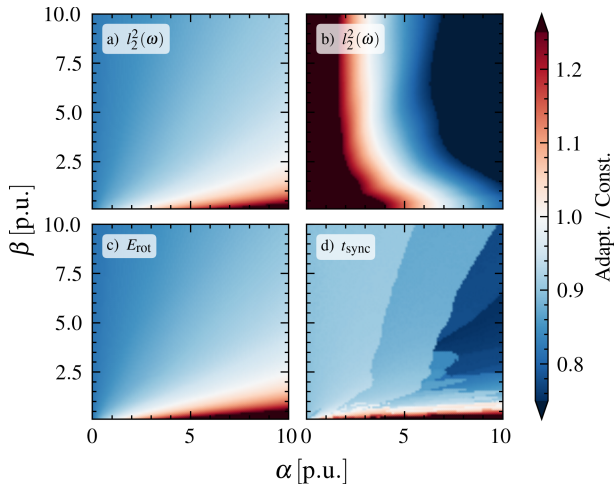


Fig. 2. a) Frequency performance measure, eq. (8), b) RoCoF performance measure, eq. (9), c) injected inertial energy, eq. (10), and d) synchronization time following a change in the power at the VSG generator indicated by the black arrow in Fig. 1, vs. the VSG parameters  $\alpha$  and  $\beta$  defined in eq. (3). Color coded are the ratio of the adaptive results to the default dispatch with only conventional generation. Blue colored areas correspond to the adaptive method performing better than the default generators.

the amplitude of oscillations of the frequency, as well as their short period components are significantly reduced by the adaptive inertia method, which is directly reflected in the frequency performance and in a reduced resynchronization time,  $t_{\text{sync,adapt}} = 16.3\text{s} < t_{\text{sync,const}} = 18.5\text{s}$ . Second, the adaptive inertia also improves the RoCoF performance measure significantly, as it quickly leads to smaller, slower oscillations of  $\dot{f}$ . Furthermore, once  $\dot{f}$  has sufficiently decreased, the lower inertia leads to even less oscillations and a fast recovery of the system in the adaptive scheme. There is a large, initial RoCoF when the faulted generator is a VSG. This is expected, since the RoCoF is inversely proportional to the inertia at the time of the fault [21], and the initial inertia  $m(t=0) = m_{\text{min}}$  is smaller in the adaptive than in the constant inertia case. That feature affects only the dynamics of the faulted generator and is not a problem as long as the latter functions purely on power electronics. In cases when  $m_{\text{min}}$  is provided by physical, electromechanically coupled inertia, or if the VSG is connected to the same bus as some conventional generation, this large initial RoCoF needs to be mitigated, however. This can be achieved by resetting the inertia to a larger value  $m(t \leq 0) > m_{\text{min}}$  once the frequency stays within some predefined range over a period of time (e.g., the frequency does not deviate more than 0.1 mHz from the synchronized state for 1 min). This adjusted adapted inertia scheme adds the benefit of greatly decreasing the initial RoCoF while not losing the advantage of the decaying inertia. In our case setting  $m_{i,\text{adapt.}}(t=0) = m_{i,\text{const.}}$  leads to a small penalty on the frequency performance measure and the energy injected while more than halving the maximum RoCoF and decreasing the RoCoF performance measure significantly (blue curves in Fig. 3). Fig. 3 finally shows the time evolution of the inertia of the faulted generator. With the adaptive scheme, the inertia

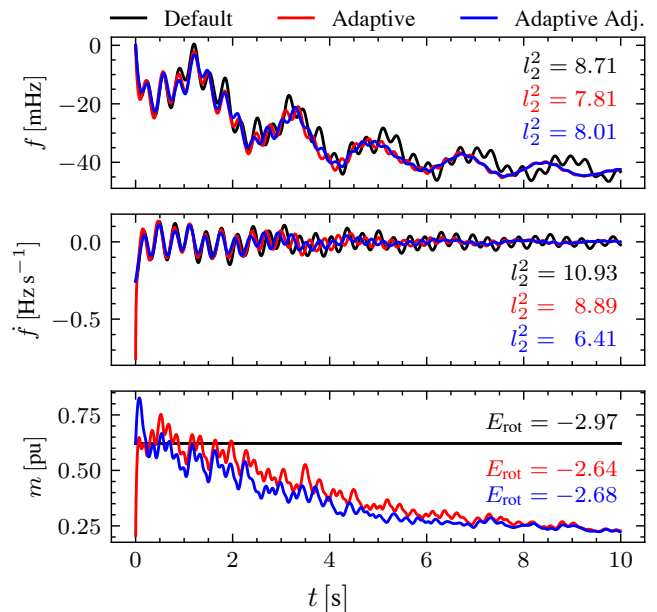


Fig. 3. Time evolution of the frequency  $f = 2\pi\omega$  (top panel), the RoCoF  $\dot{f} = 2\pi\dot{\omega}$  (middle panel), and the inertia (bottom panel) following a change of  $\delta P = -1\text{ pu}$  at the VSG indicated by the black arrow in Fig. 1. The black line corresponds to the default case with only conventional generation. The red line corresponds to the scenario with six generators being equipped with our adaptive method. The blue line corresponds to the adaptive scenario adjusted with an initial inertia of the VSGs set to the value of the default case.

shoots up right after the fault and then decays back to its minimal value. Our adaptive inertia scheme is successful at quickly reducing the RoCoF and outperforms the constant inertia method.

Interestingly, we observe that our method leads to a more homogeneous response as evaluated by the coherency measure

$$l_2^2(\text{coh}) = \sum_i \int_0^\infty (\omega_i(t) - \bar{\omega}_{\text{area}}(t))^2 dt, \quad (11)$$

where  $\bar{\omega}_{\text{area}}(t)$  is the mean frequency in the area of the RTS-96 network corresponding to node  $i$ . A smaller performance measure corresponds to a more coherent response within each area. We find that the coherence measure for the adaptive case is only 70% of the measure for the constant case. This means that the adaptive inertia not only decreases inter-area oscillations, but also intra-area, machine-machine oscillations.

Finally, we found, but do not show, that similar conclusions can be drawn for a fault on one of the conventional generators, i.e., away from any VSG. Repeating the analysis for a 1 pu fault on the generator marked by the red arrow in Fig. 1, we find that the results for the frequency performance measure as well as the energy and synchronization time resemble closely panels a, c, and d of Fig. 2. For the RoCoF performance measure we observe a small improvement from the default to the adaptive case in a large part of the parameter range. The size of the improvement is however much smaller than the one shown in Fig. 2. This is not

surprising as the RoCoF performance is mostly determined by local, short-time dynamics.

### B. PanTaGruEl

Next we investigate the effect of the adaptive inertia on a large-scale transmission grid. PanTaGruEl is a model of the European high voltage power grid that consists of 3809 nodes and 7343 lines [19], [20]. We use a dispatch where 448 nodes are generators. We promote 25% randomly chosen generators to VSGs with adaptive inertia. Those generators are homogeneously distributed over the grid and their minimum inertia is set at one third of the original inertia. We choose  $\alpha = \beta = 10$  pu which according to Fig. 2 is expected to yield significant performance improvement. In the previous section we focused on the effect of our adaptive method when the power change occurs at one of the VSGs that are equipped with the adaptive inertia. In this section we want to investigate the effect on the overall stability of the grid when a fault occurs at a conventional generator. This is motivated by the much larger scale of PanTaGruEl compared to the RTS-96 grid, and the fact that only a minority of generators can be promoted to VSGs. Of particular interest is to determine if the significantly improved network performances discussed in the previous section persist when the distance between faulted generation and VSGs grows.

We simulate instantaneous power losses of 100 MW on each conventional generator with  $P_i^0 \geq 100$  MW. The performance measures are shown in Fig. 4 for 259 individual faults on each such generator. It is clearly visible that our adaptive inertia scheme outperforms the constant inertia case almost always: it needs approximately 15% less energy to stabilize the grid, while resynchronizing faster in 91% of the cases. We have found that the RoCoF performance measure varies over three orders of magnitude. This is so because the RoCoF is a very local measure: faults on weakly connected generators with low inertia give rise to much larger RoCoF values compared to faults on large power plants in very densely connected areas. Nonetheless, we find that in 92% of all cases, the RoCoF performance measures improves. There is only one case where the performance measure decreases by more than 20%, corresponding to a fault on a strongly connected generator with several other conventional generators nearby.

A question that naturally arises is where limited resources of adaptive inertia should be located in priority. The fact that our VSGs do not improve the RoCoF performance when the fault is located in a tightly connected area of the grid suggests that performances are better when VSGs are distributed in peripheral regions. This is in contrast to previous results for conventional generators that proposed a geographically homogeneous distribution of constant, time-independent inertia [22], [23]. To test this hypothesis we investigate two different distributions of 36 VSGs geographically distributed (i) over peripheral areas (Iberian Peninsula and Balkans) and (ii) homogeneously across the grid. We made sure that the minimum amount of inertia in the grid is

the same in both cases. The results are presented in Fig. 5. While the homogeneous distribution performs slightly better for faults on the central generators, it is outperformed by the peripheral distribution for faults on peripheral generators. This confirms our conjecture that VSGs have the strongest impact when located in peripheral areas. Interestingly, these are also the areas where the modes driving the east-west inter-area oscillations in the system are located [24]. This suggests that the adaptive method can also improve the damping of these inter-area oscillations.

## VI. CONCLUSION

Guaranteeing the dynamic stability of low-inertia electric power grids is one of the main challenges facing future power systems. Motivated by the ambivalent nature of inertia, we proposed an innovative adaptive inertia scheme for virtual synchronous generators. We showed that, unlike previously suggested virtual inertia schemes, it is always stable and that, moreover, it outperforms the electromechanical inertia from conventional generators for both short- and long-time effects, regardless of the location of the considered fault. We provided numerical evidences that VSGs with adaptive inertia should be located in peripheral areas in priority to optimally enhance grid stability. As a matter of fact, our results suggest that our adaptive inertia scheme not only performs better than conventional inertia, but is also able to damp longer-range and -time inter-area oscillations. Future works should investigate this aspect in more detail.

## VII. ACKNOWLEDGMENT

We thank María Martínez-Barbeito, Pere Colet, and Damià Gomila for discussions on the optimal placement of adaptive inertia. We thank Florian Dörfler and Laurent Pagnier for general discussions on the topic.

## REFERENCES

- [1] European Commission. Joint Research Centre., *CO2 Emissions of All World Countries :JRC/IEA/PBL 2022 Report*. LU: Publications Office, 2022. [Online]. Available: <https://data.europa.eu/doi/10.2760/730164>
- [2] F. Milano, F. Dörfler, G. Hug, D. J. Hill, and G. Verbič, “Foundations and Challenges of Low-Inertia Systems (Invited Paper),” in *2018 Power Systems Computation Conference (PSCC)*, Jun. 2018, pp. 1–25.
- [3] F. Paganini and E. Mallada, “Global performance metrics for synchronization of heterogeneously rated power systems: The role of machine models and inertia,” in *2017 55th Annual Allerton Conference on Communication, Control, and Computing (Allerton)*, Oct. 2017, pp. 324–331.
- [4] K. Creighton, M. McClure, R. Skillen, and A. Rogers, “Increased Wind Generation in Ireland and Northern Ireland and the Impact on Rate of Change of Frequency,” in *Proceedings of the 12th Wind Integration Workshop*, 2013, p. 6. [Online]. Available: <http://www.eirgridprojects.com/site-files/library/EirGrid/Increased%20Wind%20Generation%20in%20Ireland%20and%20Northern%20Ireland%20and%20the%20Impact%20on%20Rate%20of%20Change%20of%20Frequency.pdf>
- [5] T. Kerci, M. Hurtado, M. Gjergji, S. Tweed, E. Kennedy, and F. Milano, “Frequency Quality in Low-Inertia Power Systems,” Feb. 2023. [Online]. Available: <http://arxiv.org/abs/2302.01630>
- [6] S. D’Arco and J. A. Suul, “Virtual synchronous machines — Classification of implementations and analysis of equivalence to droop controllers for microgrids,” in *2013 IEEE Grenoble Conference*, Jun. 2013, pp. 1–7.

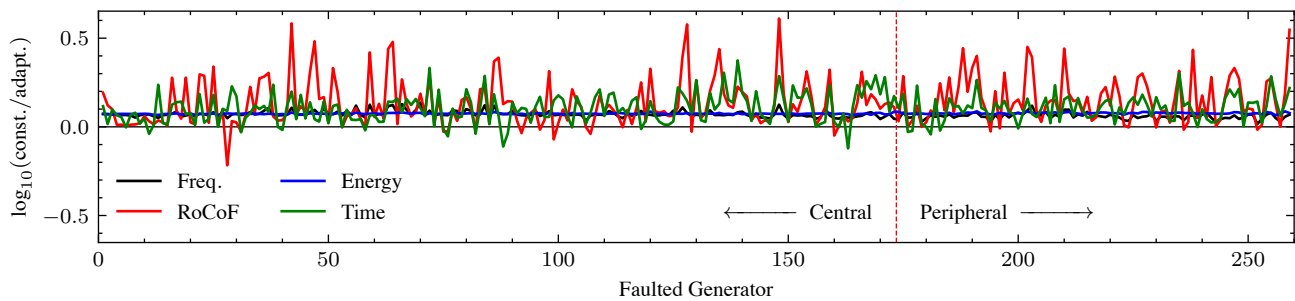


Fig. 4. Ratio of the four performance measures with constant inertia only vs. with adaptive inertia (112 VSGs), on a log-scale. The red dashed line separates the faulted generator location into central (on the left) and peripheral (on the right).

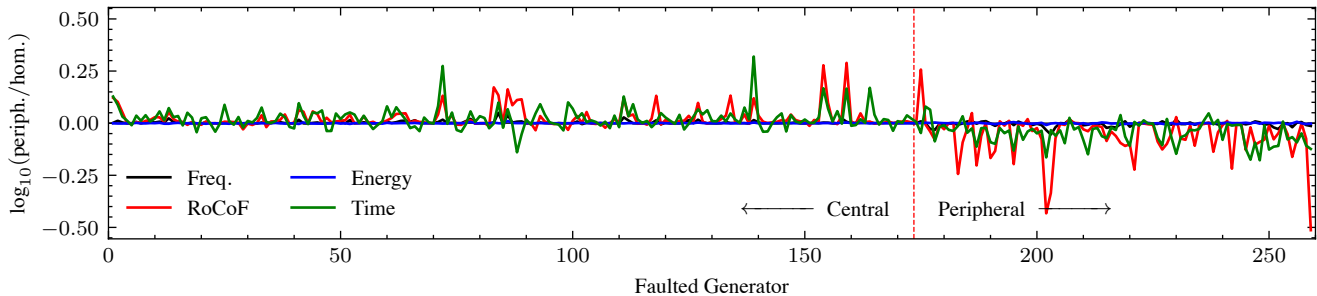


Fig. 5. Ratio of the four performance measures with 36 VSGs distributed in the periphery (Iberian Peninsula and Balkans) vs. homogeneously on the grid, on a log-scale. The red dashed line separates the faulted generator location into central (on the left) and peripheral (on the right).

- [7] W. Sang, W. Guo, S. Dai, C. Tian, S. Yu, and Y. Teng, "Virtual Synchronous Generator, a Comprehensive Overview," *Energies*, vol. 15, no. 17, p. 6148, Aug. 2022. [Online]. Available: <https://www.mdpi.com/1996-1073/15/17/6148>
- [8] M. A. Torres L., L. A. C. Lopes, L. A. Morán T., and J. R. Espinoza C., "Self-Tuning Virtual Synchronous Machine: A Control Strategy for Energy Storage Systems to Support Dynamic Frequency Control," *IEEE Transactions on Energy Conversion*, vol. 29, no. 4, pp. 833–840, Dec. 2014.
- [9] D. Li, Q. Zhu, S. Lin, and X. Y. Bian, "A Self-Adaptive Inertia and Damping Combination Control of VSG to Support Frequency Stability," *IEEE Transactions on Energy Conversion*, vol. 32, no. 1, pp. 397–398, Mar. 2017.
- [10] J. Alipoor, Y. Miura, and T. Ise, "Power System Stabilization Using Virtual Synchronous Generator With Alternating Moment of Inertia," *IEEE Journal of Emerging and Selected Topics in Power Electronics*, vol. 3, no. 2, pp. 451–458, Jun. 2015.
- [11] F. Wang, L. Zhang, X. Feng, and H. Guo, "An Adaptive Control Strategy for Virtual Synchronous Generator," *IEEE Transactions on Industry Applications*, vol. 54, no. 5, pp. 5124–5133, Sep. 2018.
- [12] A. Kasis, S. Timotheou, and M. Polycarpou, "Stability of power networks with time-varying inertia," in *2021 60th IEEE Conference on Decision and Control (CDC)*, Dec. 2021, pp. 2788–2793.
- [13] —, "On the stability properties of power networks with time-varying inertia," Jan. 2023. [Online]. Available: <http://arxiv.org/abs/2301.09202>
- [14] Y. Liu and C. Shen, "Equivalent Inertia Provided by Droop Control of Fast Frequency Regulation Resources," Dec. 2022. [Online]. Available: <http://arxiv.org/abs/2212.00685>
- [15] J. Machowski, Z. Lubosny, J. W. Bialek, and J. R. Bumby, *Power System Dynamics: Stability and Control*, 3rd ed. Hoboken, NJ, USA: John Wiley, 2020.
- [16] A. R. Bergen and V. Vittal, *Power Systems Analysis*, 2nd ed. Upper Saddle River, NJ: Prentice Hall, 2000.
- [17] A. Bergen and D. Hill, "A Structure Preserving Model for Power System Stability Analysis," *IEEE Transactions on Power Apparatus and Systems*, vol. PAS-100, no. 1, pp. 25–35, Jan. 1981.
- [18] C. Grigg, P. Wong, P. Albrecht, R. Allan, M. Bhavaraju, R. Billinton, Q. Chen, C. Fong, S. Haddad, S. Kuruganty, W. Li, R. Mukerji, D. Patton, N. Rau, D. Reppen, A. Schneider, M. Shahidehpour, and C. Singh, "The IEEE Reliability Test System-1996. A report prepared by the Reliability Test System Task Force of the Application of Probability Methods Subcommittee," *IEEE Transactions on Power Systems*, vol. 14, no. 3, pp. 1010–1020, Aug. 1999.
- [19] L. Pagnier and P. Jacquod, "Inertia location and slow network modes determine disturbance propagation in large-scale power grids," *PLOS ONE*, vol. 14, no. 3, p. e0213550, Mar. 2019. [Online]. Available: <https://journals.plos.org/plosone/article?id=10.1371/journal.pone.0213550>
- [20] M. Tyloo, L. Pagnier, and P. Jacquod, "The key player problem in complex oscillator networks and electric power grids: Resistance centralities identify local vulnerabilities," *Science Advances*, vol. 5, no. 11, p. eaaw8359, Nov. 2019. [Online]. Available: <https://advances.sciencemag.org/content/5/11/eaaw8359>
- [21] R. Delabays, M. Tyloo, and P. Jacquod, "Rate of change of frequency under line contingencies in high voltage electric power networks with uncertainties," *Chaos: An Interdisciplinary Journal of Nonlinear Science*, vol. 29, no. 10, p. 103130, Oct. 2019. [Online]. Available: <https://aip.scitation.org/doi/full/10.1063/1.5115002>
- [22] L. Pagnier and P. Jacquod, "Optimal Placement of Inertia and Primary Control: A Matrix Perturbation Theory Approach," *IEEE Access*, vol. 7, pp. 145 889–145 900, 2019.
- [23] B. K. Poolla, S. Bolognani, and F. Dörfler, "Placing Rotational Inertia in Power Grids," in *2016 American Control Conference (ACC)*, Jul. 2016, pp. 2314–2320.
- [24] J. Fritzsche and P. Jacquod, "Long Wavelength Coherency in Well Connected Electric Power Networks," *IEEE Access*, vol. 10, pp. 19 986–19996, 2022.